Electrical Power and Energy Systems 64 (2015) 221–232

Contents lists available at ScienceDirect

Electrical Power and Energy Systems

journal homepage: www.elsevier.com/locate/ijepes

Real power and frequency control of a small isolated power system

Srinivasa Rao Gampa, Debapriya Das *

Department Electrical Engineering, Indian Institute of Technology, Kharagpur 721302, India

ARTICLE INFO

Article history:
Received 15 May 2013
Received in revised form 25 June 2014
Accepted 6 July 2014

Keywords:
Wind turbine generator
Diesel generator
P–I controller
P–I–D controller
Genetic algorithm
Particle swarm optimization

ABSTRACT

This paper describes the dynamic analysis of a small isolated power system comprising a wind turbine generator and a diesel generator. The analysis is carried out in time domain considering simplified models of the system components by taking into account the wind turbine pitch controller and the diesel engine speed governor. Wind disturbance model consisting components of gusting of wind, rapid ramp changes and random noise. The wind generator is always operated with its rated power and the additional power required by the load is supplied by the diesel generator. For better dynamic performances of wind–diesel system under wind and load disturbance conditions, two control schemes are used. In the first case, a proportional–integral (P–I) controller and in the second case a proportional–integral–derivative (P–I–D) controller are used. Gain parameters of these controllers are optimized using genetic algorithm (GA) and Particle swarm optimization (PSO) considering two different objective functions and the results are compared. The sensitivity analysis of the wind diesel system is carried out for parameter uncertainties and the stability of the system is analyzed using D-stability criterion. Analysis is also carried out to examine the effect of power injection to a 69 bus radial distribution network by wind–diesel isolated system.

Introduction

With the rapid depletion of fossile fuels the role of renewable energy resources is increasing in the current world energy scenario. Wind power generation is most economical compared to other nonconventional energy resources. Wind turbine generators (WTG's) are mainly suitable for isolated loads where the power transmission is a major problem. In remote areas generally electrical energy has been supplied by diesel generators. The wind–diesel isolated power system is most popular for remote areas. Diesel generator functions as a backup source to compensate the power supply variations due to wind speed fluctuations. High power fluctuations results at the output of wind turbines due to sudden changes in load and abnormal wind speed variations and they should be minimized. A number of conventional methods such as state space method, optimal control and robust control are found in the literature to control WTG output power. The objective is to achieve good dynamic performance of WTG output power under wind and load disturbance conditions. Scott et al. [1] have studied the dynamic behavior of an autonomous system comprising of diesel generator and wind turbine generators. Their analysis reveals that the change in control system settings can improve the damping. Kamwa [2] studied the dynamic modeling and performance of wind–diesel systems by applying a programmable smoothing-load and using a standard PID regulator installed on the diesel unit. Tripathy et al. [3] have used magnetic energy storage unit to minimize the power and frequency deviations under load disturbance conditions in the isolated wind–diesel power system. Kariniotakis and Stavrakakis [4,5] have studied the autonomous wind–diesel system under various scenarios. They have presented the mathematical model as well as implementation of their algorithm. Das et al. [6] have studied the dynamic performance of an isolated wind–diesel hybrid power system. Chedid et al. [7] have used fuzzy logic controller for an isolated wind–diesel hybrid power system. However fuzzy logic controller for such system depends extensively on heuristic knowledge. Papathanassiou and Papadopoulos [8] have integrated the analysis of main modes of the wind–diesel hybrid system and the parameters of the controllers. Above literature review shows that the dynamic behavior of wind–diesel power system has been the subject of many researchers [1–8] dealing with small autonomous installation but most of the literatures mentioned above did not consider the details of modeling of wind speed and power [2,3,6–8].

Previous researchers have also not made any attempt to optimize the gain parameters of the controller to improve the dynamic performances of the wind–diesel system to withstand wind disturbance. In addition to that they have not studied the

* Corresponding author.
E-mail address: ddas@ee.iitkgp.ernet.in (D. Das).

http://dx.doi.org/10.1016/j.ijepes.2014.07.037
0142-0615/

Nomenclature

C_p	coefficient of wind turbine power
$MGWS$	maximum gust wind speed (m/s)
$MRWS$	maximum ramp wind speed (m/s)
ω_B	angular velocity of blade (mech rad/s)
γ	tip speed ratio (m/rad)
β	blade pitch angle (degrees)
P_{max}	wind turbine generator setpoint
P_{wtg}	wind turbine generator power (kW)
P_w	mechanical power of wind turbines (kW).
V_w	total wind velocity (m/s)
V_{WB}	constant wind component (m/s)
V_{WG}	wind component of gust disturbance(m/s)
V_{WR}	wind component ramp disturbance (m/s)
V_{WN}	wind component of random noise (m/s)
T_{gust_1}	gust starting time (s)
T_{gust}	gust period (s)
T_{ramp_1}	ramp start time (s)
T_{ramp_2}	ramp maximum time (s)
T_d	time delay
c_1, c_2	acceleration of the swarm
r_1, r_2	random numbers in between 0 and 1
x_i^k	position of ith particle at kth iteration
x_i^{k+1}	position of ith particle at $(k+1)$th iteration
v_i^k	velocity of ith particle at kth iteration
v_i^{k+1}	velocity of ith particle at $(k+1)$th iteration
$pbest_i^k$	best position of ith particle
$gbest^k$	best position of the swarm
w^k	inertia weight of kth iteration
w_{max}	maximum value of the inertia
w_{min}	minimum value of the inertia
$iter_k$	value of the kth iteration
$iter_{max}$	value of the maximum iteration
IT	generation number
ITMAX	maximum number of generations

effect of power injection by wind–diesel system into a distribution network.

In power systems P–I–D controller is generally used in the design of power system stabilizers and load frequency control applications to improve the dynamic responses of the system [9–12]. In this paper, two control schemes are used to control the blade pitch angle of the wind turbine generator for obtaining the better dynamic performances of wind–diesel hybrid system under wind disturbance conditions. The first controller is a proportional–integral (P–I) controller and second one is proportional–integral–derivative (P–I–D) controller. Gain parameters of these two controllers are optimized using genetic algorithm (GA) and Particle swarm optimization (PSO) considering the two different objective functions. The sensitivity analysis and stability analysis of wind diesel system are studied to test the robustness of the closed loop system for parameter variations. Finally, the power injection by the wind diesel system into 69 node distribution network is also examined.

Modeling of wind speed and power

Model of wind speed

A wind disturbance model is considered to study the dynamic performance of wind–diesel system. The wind disturbance is modeled considering the sum of base wind, gusting, ramp, and random noise. The generated power of the wind turbine generator depends on wind speed (V_W). The mathematical model for different wind speed components are discussed below in detail [13].

The four component wind model is described by using the following equation:

$$V_W = V_{WB} + V_{WG} + V_{WR} + V_{WN} \tag{1}$$

The base wind mathematical model is expressed by

$$V_{WB} = K_B \tag{2}$$

where K_B is a constant and this component of wind is constant component present in the model of wind speed.

The gust wind mathematical model is expressed by

$$V_{WG} = \begin{cases} 0 & \text{for } t < T_{gust_1} \\ V_{cos} & \text{for } T_{gust_1} < t < T_{gust_1} + T_{gust} \\ 0 & \text{for } t > T_{gust_1} + T_{gust} \end{cases} \tag{3}$$

where 't' is time in seconds and,

$$V_{COS} = (MGWS/2)(1 - cos(2\pi[(t/T_{gust}) - (T_{gust_1}/T_{gust})])) \tag{4}$$

The ramp wind mathematical model is expressed by

$$V_{WR} = \begin{cases} 0 & \text{for } t < T_{ramp_1} \\ V_{ramp} & \text{for } T_{ramp_1} < t < T_{ramp_2} \\ 0 & \text{for } t > T_{ramp_2} \end{cases} \tag{5}$$

where

$$V_{ramp} = MRWS(1 - (t - T_{ramp_2})/(T_{ramp_1} - T_{ramp_2})) \tag{6}$$

where $T_{ramp_2} > T_{ramp_1}$. This equation can be approximated to a step change by minimizing the difference between T_{ramp_2} and T_{ramp_1}.

The noise wind model is expressed by

$$V_{WN} = 2\sum_{i=1}^{N}[S_V(\Omega_i)\Delta\Omega]^{1/2} cos(\Omega_i t + \phi_i) \tag{7}$$

where

$$\Omega_i = (i - 1/2)\Delta\Omega \tag{8}$$

ϕ_i = a random variable with uniform probability density on the interval 0–2π and $S_V(\Omega_i)$ is the spectral density function defined as

$$S_V(\Omega_i) = \frac{2K_N F^2|\Omega_i|}{\pi^2[1 + (F\Omega_i/\mu\pi)^2]^{4/3}} \tag{9}$$

where

K_N = surface drag coefficient = 0.004
F = turbulence scale = 2000 m
Ω_i = ith frequency component of random noise
μ = mean speed of wind = 7.5 m/s

Here N is considered as 50.

The four components together are considered for analyzing the dynamics of the wind–diesel hybrid system.

Wind generator output power

The wind turbine generator characterized by the power coefficient C_p and wind velocity. The power coefficient C_p is again characterized by tip speed ratio and blade pitch angle. The wind blade dynamics are approximated by the following non linear functions.

Tip speed ratio is expressed by

$$\gamma = \frac{V_W}{\omega_B} \tag{10}$$

The power coefficient C_p can be approximated by

$$C_p = \frac{1}{2}(\gamma - 0.0228\beta^2 - 5.6)e^{-0.17\gamma} \tag{11}$$

The wind power is expressed by

$$P_W = \frac{1}{2}\rho A_B C_p V_W^3 \tag{12}$$

The air density of the wind is ρ (= 1.25 kg/m^3) and the area swept by the wind blade is A_B (= 1735 m^2).

Fig. 1 represents the characteristic curve of wind speed versus WTG power. The cut in velocity is the wind speed at which the wind turbine starts delivering wind power.

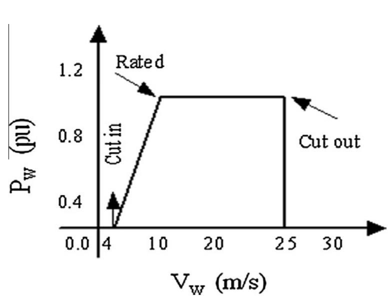

Fig. 1. Wind speed versus wind power.

Model of wind–diesel system

The wind–diesel hybrid model consists of the following sub systems [1,3,6].

1. Wind speed model
2. Diesel generator model
3. Control scheme for WTG power
4. Wind turbine generator model

During the start up and synchronization, a minimum wind speed is required. The diesel generator dynamics are controlled by diesel speed control governor.

Fig. 2 represents the conceptual model of the wind–diesel isolated power system. The uncertainty in the wind speed is modeled considering gust, ramp and random noise. The mathematical model of wind speed has been discussed in the previous section. The diesel generator drives the synchronous generator and develops the reference grid for the induction generator which is coupled to the wind turbine. The wind turbine generator output power can be controlled by changing the pitch angle of the blades of the wind turbine generator using a hydraulic pitch actuator. When the wind power exceeds the reference value the pitch of the blade is controlled to bring the power generated by WTG is equal to the set point.

State space model of wind–diesel system

A linearized model of WTG and diesel generator is considered to analyze the dynamic performances under wind speed and load fluctuations. The state space model of the wind–diesel hybrid system (Fig. 3) can be written as follows

$$\dot{X} = AX + \Gamma P \tag{13}$$

where X and P are state and disturbance vectors respectively. A and Γ are constant matrices associated with wind–diesel hybrid system.

$$X' = [\Delta H_1\ \Delta H\ \Delta D\ \Delta\omega_1\ \Delta\omega_2\ \Delta P_{f_1}\ \Delta P_{f_2}\ \Delta U_1] \tag{14}$$

$$P' = [P_W P_{load} P_{\max}] \tag{15}$$

where X' and P' are transposes of X and P respectively. ΔH_1, ΔH, ΔD, $\Delta\omega_1$, $\Delta\omega_2$, ΔP_{f_1}, ΔP_{f_2} and ΔU_1 are state variables X_1, X_2, X_3, X_4, X_5, X_6, X_7 and X_8 respectively.

$$\Delta P = P_{\max} - P_{wtg} \tag{16}$$

$$P_{wtg} = K_{fc}(\Delta\omega_1 - \Delta\omega_2) \tag{17}$$

where $\Delta\omega_1$ and $\Delta\omega_2$ are angular frequency deviations of wind turbine generator and diesel generator and K_{fc} is the fluid coupling coefficient. Block diagram representation of wind diesel isolated power system is shown in Fig. 3. In this paper P–I and P–I–D control schemes are used to actuate the hydraulic pitch actuator to control the wind turbine blade pitch angle to adjust the wind turbine power according to the set point. The diesel generator supplies the additional power required by the load. The hydraulic pitch actuator generates the necessary control signal to adjust the wind turbine blade pitch angle to control the power of WTG.

The hydraulic pitch actuator transfer function is given as

$$\frac{\Delta H(s)}{\Delta U(s)} = \frac{K_{hp_2}(1 + sT_{hp_1})}{(1 + sT_{hp_2})(1 + s)} \tag{18}$$

In the first control scheme, only Proportional Integral controller is used by setting $K_3 = 0$ in Fig. 3. and in the second control scheme P–I–D controller is used. In both the cases the gains are optimized by using genetic algorithm and particle swarm optimization. The transfer function of Eq. (18) can be split into two blocks by considering ΔH_1 as state variable X_1, i.e.,

$$\frac{\Delta H_1(s)}{\Delta U(s)} = \frac{1}{(1 + sT_{hp_2})} \tag{19}$$

$$\frac{\Delta H(s)}{\Delta H_1(s)} = \frac{K_{hp_2}(1 + sT_{hp_1})}{(1 + s)} \tag{20}$$

and

$$\frac{\Delta D(s)}{\Delta H(s)} = \frac{K_{hp_3}}{(1 + s)} \tag{21}$$

The transfer function of diesel generator governor can be represented by

$$\frac{\Delta P_{f_2}(s)}{\Delta\omega(s)} = \frac{K_d(1 + s)}{s(1 + sT_1)} \tag{22}$$

Eq. (22) can be split into two blocks by considering ΔP_{f_1} as another state variable.

$$\frac{\Delta P_{f_1}(s)}{\Delta\omega(s)} = \frac{K_d}{s} \tag{23}$$

$$\frac{\Delta P_{f_2}(s)}{\Delta P_{f_1}(s)} = \frac{(1 + s)}{(1 + sT_1)} \tag{24}$$

The data are given in Appendix A.

Gain parameters optimization of P–I and P–I–D controllers using GA

Genetic algorithm (GA) is quite popular to solve the optimization problems mainly because of its robustness in finding optimal solution and ability to provide near optimal solution. Genetic algorithms employ search procedures based on the mechanics of

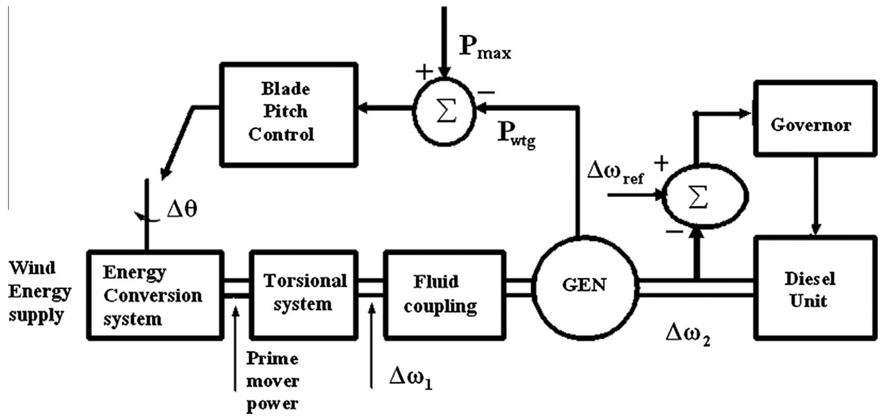

Fig. 2. Conceptual block diagram of wind–diesel isolated power system.

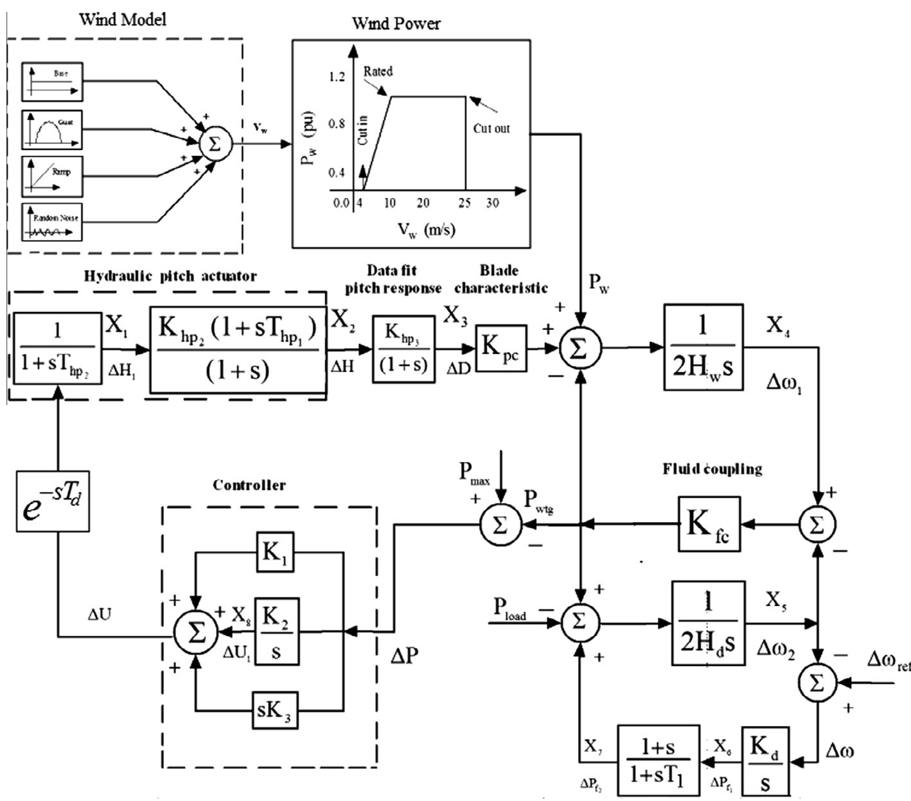

Fig. 3. Wind–diesel small isolated power system.

natural selection and survival of the fittest. It has been applied to several power system problems. In GA, the performance of each binary string in the population is measured by calculating its fitness value, which is to be maximized to get the optimal solution. It is associated with the objective function to be minimized in the optimization procedure [14,15].

Fitness function based on eigenvalues

The eigenvalues of wind–diesel isolated system matrix A are the roots of the characteristic equation, i.e.,

$$|A - \lambda I| = 0 \tag{25}$$

where the values of the λ are the eigenvalues of the matrix A and I is the identity matrix of the same order as that of A. The system will be stable if all the eigenvalues lie on the left half of the s-plane. When all the eigenvalues lie on the left half of the s-plane, the system stability mainly depends on the eigenvalue nearer to the origin. For better dynamic performances it must be forced to move away from the origin on the left half of the s-plane. Mathematically, when all the eigenvalues lie on the left half of the s-plane, the eigenvalue whose real part is close to the origin, we define,

$$\zeta = max(real(\lambda_i)); \quad i = 1, 2, 3, \ldots, n \tag{26}$$

where ζ is known as degree of stability. In this case the objective function is defined as

$$J_1 = |\zeta| \tag{27}$$

and J_1 has to be maximized. As mentioned earlier fitness need to be maximized in GA therefore, fitness function F_1 is given as:

$$F_1 = J_1 \tag{28}$$

Fitness function based on quadratic objective function

In this case an objective function

$$J_2 = \int_0^t (P_{\max} - P_{wtg})^2 dt \tag{29}$$

is minimized for obtaining the optimum gain parameters of P–I and P–I–D controllers using GA and the fitness function is defined as:

$$F_2 = \frac{K}{1 + J_2} \tag{30}$$

where K is considered as 100.

Constraints on gain parameters

For the system shown in Fig. 3 limits are imposed on proportional, integral and derivative gain parameters i.e.

$$K_i^{\min} \leqslant K_i \leqslant K_i^{\max}; \quad i = 1, 2, 3 \tag{31}$$

K_1, K_2 and K_3 will always lie in between their specified minimum and maximum values and can be obtained as:

$$K_i = K_i^{\min} + \frac{(K_i^{\max} - K_i^{\min})}{(2^{l_i} - 1)} I_i \tag{32}$$

where l_i = bit size of K_i and I_i is decimal value of K_i after converting each binary string. Same bit size is chosen for K_1, K_2 and K_3, and while optimizing P–I gain settings K_3 was not considered.

Algorithm for GA based optimization

Complete algorithm is given below:

Step-1
Generate binary strings and initialize population
(a) $[K_1, K_2]$ for P–I controller.
(b) $[K_1, K_2, K_3]$ for P–I–D controller.
Where K_1, K_2 and K_3 represent the binary substrings
Step-2
(a) Calculate the decimal value of each binary substring in a string to obtain the values of K_1 and K_2 for P–I controller and K_1, K_2 and K_3 for P–I–D controller using Eq. (32).
(b) Obtain the eigenvalues of the system given by Eq. (25) and determine the fitness for P–I and P–I–D controllers using Eq. (28).
(c) Solve Eq. (13) for obtaining the fitness value considering P–I and P–I–D controllers using Eq. (30).
Step-3
Set IT = 1.
Step-4
For j = 1 to j = "population size × cross over rate", Do;
(a) Using Roulette wheel selection method, select two parents from population.
(b) Generate two off springs by performing cross over.
(c) Based on mutation probability mutate these two offspring.
(d) Generate new population combining newly generated strings and strings having best fitness from old population.
Step-5:
Calculate fitness of each offspring (as in **Step-2**)
IT = IT + 1
If (IT ⩽ ITMAX) go to **Step-4**.

Gain parameters optimization of P–I and P–I–D controllers using PSO

Particle swarm optimization (PSO) is a metaheuristic optimization technique which starts with a randomly generated population called swarm. The swarm consists of individuals called particles and each particle in the swarm represents a potential solution of the optimization problem. Each particle moves in a multidimensional search space with a velocity guided by the information of the objective function. The velocity and position of each particle are updated according to the following equations:

$$v_i^{k+1} = w^k v_i^k + c_1 r_1 \left(pbest_i^k - x_i^k\right) + c_2 r_2 \left(gbest^k - x_i^k\right) \tag{33}$$

$$v_i^{\min} \leqslant v_i^k \leqslant v_i^{\max} \tag{34}$$

$$w^k = w_{\max} - \frac{(w_{\max} - w_{\min})}{iter_{\max}} iter_k \tag{35}$$

$$x_i^{k+1} = x_i^k + v_i^{k+1} \tag{36}$$

where c_1 and c_2 are positive acceleration constants and both the values are set to 1.5. The values of r_1 and r_2 are randomly generated numbers in between 0 and 1. In the Eq. (33) the second term represents the cognitive part of PSO where the particle changes its velocity based on its own experience and memory and the third term represents the social part of PSO where the particle changes its velocity based on the knowledge adapted by the social behavior of the neighborhood particles in the swarm. In the PSO algorithm the parameter $v_i^{\max}$ determines the resolution or fitness between which regions the present position and target position are searched. If $v_i^{\max}$ is too high the particles may fly past good solutions and if it is too low the particles may not explore beyond local solutions and hence the value of $v_i^{\max}$ is often chosen within 10–20% of the dynamic range of the variable. The inertia weight (w) provides a balance between global and local explorations. As originally developed, w often decreases linearly from about 0.9 to 0.4 the values of $w_{\max}$ and $w_{\min}$ are set to 0.9 and 0.4 respectively [9,16].

Optimization of P–I and P–I–D controller gains using PSO

For finding the optimum gain parameters of P–I and P–I–D controller for the wind diesel system using PSO the same objective functions described by Eqs. (27) and (29) developed based on eigenvalue and quadratic objective function in the previous section are considered. The optimum gains are obtained by maximizing the fitness functions described by Eqs. (28) and (30) using PSO.

Algorithm for PSO based optimization

The complete algorithm for PSO is given below:

Step-1
Initialize the population of particles of the swarm with random positions and set initial velocity positions to zero,
(a) $[K_1, K_2]$ for P–I controller.
(b) $[K_1, K_2, K_3]$ for P–I–D controller.
Where K_1, K_2 and K_3 represent individual particles in the swarm.

Step-2
Set iter = 1.
Step-3
(a) Calculate the fitness value of each particle using Eq. (28) for P–I controller and using Eq. (30) for P–I–D controller.

(b) If the fitness value of particle is better than pbest, set the current value as pbest.
(c) The best fitness value of pbest is identified as gbest.

Step-4
(a) Calculate the velocities of the particles using Eqs. (33)–(35).
(b) Update the positions of the particles using Eq. (36).

Step-5
Iter = Iter + 1;
If (iter ⇐ iter$_{max}$) go to **Step-3**

Results and discussions

The parameters of P–I and P–I–D controllers are optimized for wind diesel system using GA and PSO techniques and the algorithms are executed using MATLAB 2007a software. The wind diesel system model is developed using MATLAB simulink for dynamic response analysis. Fig. 4a shows the MATLAB simulink model developed for wind diesel system. In Figs. 4b and 4c wind speed model and hydraulic pitch actuator are shown respectively which are subsystems of Fig. 4a.

Performance of GA based P–I and P–I–D controllers

Table 1 depicts the optimum values of P–I and P–I–D gain parameters obtained using GA and the optimum value of objective function Eq. (27). From Table 1, it is seen that the value of J_1 with P–I–D controller is slightly better than that obtained with P–I controller.

Table 2 depicts the optimum values of P–I and P–I–D gain parameters and the optimum value of objective function Eq. (29) using GA. In this case P_{max} was set to 0.6 pu and total load demand P_{load} was considered as 1.0 pu. For different values of P_{max}, the P–I and P–I–D gain parameters were also optimized and it was found that these gain parameters are more or less close to the values given in Table 2. Therefore it may be concluded that the optimum values of gain parameters are more or less same for $0 \leqslant P_{max} \leqslant 0.6$.

From Table 2, it is observed that the value of J_2 with optimum P–I–D controller is much lower than that obtained with optimum P–I controller. Tables 3 and 4 gives the eigenvalues of the system without any controller, with optimum P–I and P–I–D controllers considering the gain values obtained using GA given in Tables 1 and 2 respectively.

Fig. 5(a)–(c) show the dynamic responses for WTG frequency deviation, WTG power output and diesel generator power output considering the optimum P–I and P–I–D gain parameters given in Table 1. These responses are obtained for P_{max} = 0.6 pu, P_{load} = 1.0 pu and it was assumed that the base wind speed was present throughout the study period, i.e., for $0 \leqslant t \leqslant 80$ s; gust wind speed was present for 5 s $\leqslant t \leqslant$ 15 s and ramp wind speed was present for 30 s $\leqslant t \leqslant$ 40 s. The noise wind component was present throughout, i.e., for $0 \leqslant t \leqslant 80$ s. It is seen from Fig. 5(a) and (c) that the peak value of WTG frequency deviation and peak value of diesel power deviation with P–I–D controller is more than that obtained with P–I controller. For wind power deviation (Fig. 5(b)) peak value is slightly less with P–I–D controller than that obtained with P–I controller. However, when ramp wind period is over (i.e., $t > 40$ s), there is a sudden drop in WTG frequency deviation, wind turbine output power and increase in diesel generator power output during transient imbalance. But when the ramp wind speed period is over, the dynamic responses (Fig. 5(a)–(c)) with P–I–D controller is much superior than that obtained with P–I controller in terms of peak deviation.

Fig. 6(a)–(c) show the dynamic responses for WTG frequency deviation, WTG power output and diesel generator power output considering the optimum P–I and P–I–D gain parameters given in Table 2 under similar conditions as mentioned above. From Fig. 6(a)–(c), it is seen that the P–I–D controller gives much better dynamic responses. By observing Figs. 5 and 6, we can see that the noise wind component has negligible effect on the dynamic responses and may be neglected from the mathematical model.

Fig. 7 shows the dynamic performances considering optimum P–I–D gain parameters (Table 1) obtained by maximizing the degree of stability and optimum P–I–D gain parameters (Table 2) obtained

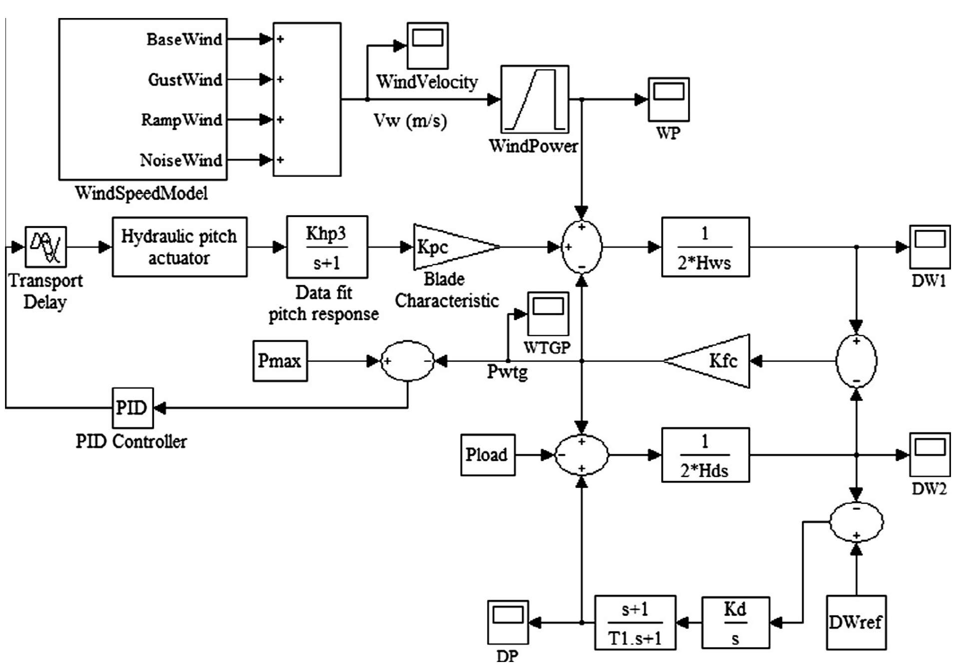

Fig. 4a. Wind–diesel small isolated power system MATLAB simulink model.

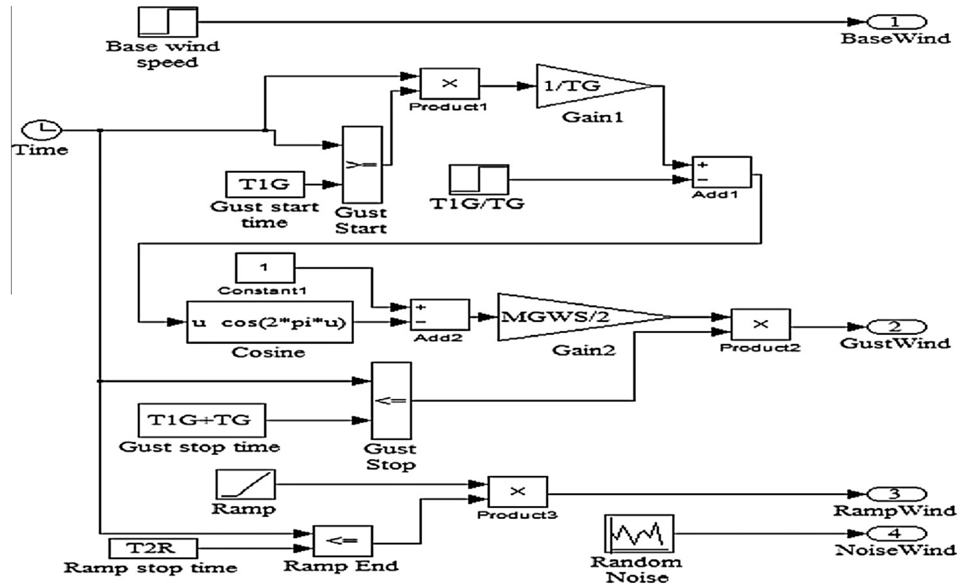

Fig. 4b. Wind speed MATLAB simulink model.

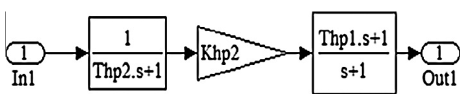

Fig. 4c. Hydraulic pitch actuator MATLAB simulink model.

Table 1
Optimized P–I and P–I–D gain parameters considering fitness function given by Eq. (28) using GA.

Control schemes	Optimum gains	Objective function (J_1)
P–I	K_1 = 51.18 K_2 = 74.12	0.4959
P–I–D	K_1 = 103.53 K_2 = 124.12 K_3 = 73.53	0.5322

Table 2
Optimized P–I and P–I–D gain parameters considering fitness function given by Eq. (30) using GA.

Control schemes	Optimum gains	Objective function (J_2)
0.5322 P–I	K_1 = 140.20 K_2 = 25.29	20.52
0.5322 P–I–D	K_1 = 197.65 K_2 = 108.82 K_3 = 50.20	12.85

Table 3
Eigenvalues of the wind–diesel system using GA with J_1.

Eigenvalues without controller	Eigenvalues with P–I controller	Eigenvalues with P–I–D controller
	$F_1 = J_1$ (Eq. (28))	$F_1 = J_1$ (Eq. (28))
−39.0283	−39.0281	−39.0383
−24.3995	−24.8216	−13.4088 ± 14.9253i
−3.4191	−2.1863	−1.6278
−1.0408 ± 0.2401i	−1.3467	−0.5372 ± 0.9059i
−0.3467 ± 0.7300i	−0.6240 ± 2.6563i	−0.5322 ± 1.0102i
–	−0.4959 ± 0.8912i	–

Table 4
Eigenvalues of the Wind–diesel system using GA with J_2.

Eigenvalues without controller	Eigenvalues with P–I controller	Eigenvalues with P–I–D controller
	$F_2 = J_2$ (Eq. (30))	$F_2 = J_2$ (Eq. (30))
−39.0283	−39.0275	−39.0357
−24.3995	−25.5599	−12.0343 ± 9.1564i
−3.4191	−1.1152 ± 4.9645i	−3.1530
−1.0408 ± 0.2401i	−1.7011	−1.7735
−0.3467 ± 0.7300i	−0.4647 ± 0.8772i	−0.4681 ± 0.8788i
–	−0.1741	−0.6554

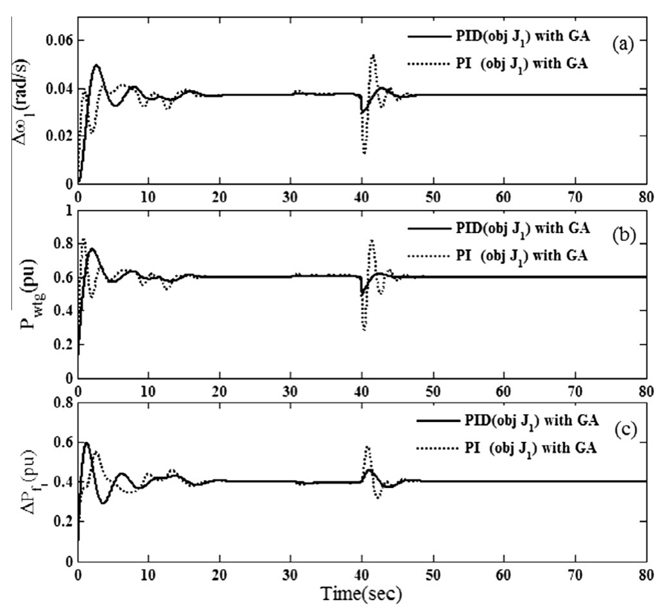

Fig. 5. Dynamic responses for (a) WTG frequency deviation, (b) WTG power output and (c) diesel generator power output considering optimum value of P–I and P–I–D gain parameters obtained using GA (Table 1).

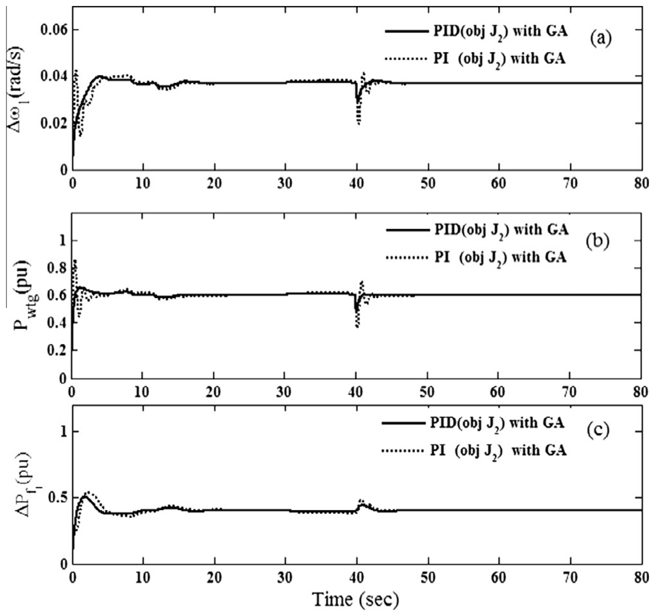

Fig. 6. Dynamic responses for (a) WTG frequency deviation, (b) WTG power output and (c) diesel generator power output considering optimum value of P–I and P–I–D gain parameters obtained using GA (Table 2).

by minimizing quadratic objective function. From Fig. 7, it is seen that the dynamic responses are better in terms of peak deviation considering optimum gain settings of P–I–D controller (see Table 2) obtained by minimizing the quadratic objective function.

Performance of PSO based P–I and P–I–D controllers

Table 5 depicts the optimum values of P–I and P–I–D gain parameters obtained using PSO and the optimum value of objective function Eq. (27). From Table 5, it is seen that the value of J_1 with P–I–D controller is slightly better than that obtained with P–I controller. Table 6 depicts the optimum values of P–I and P–I–D gain parameters and the optimum value of objective function Eq. (29)

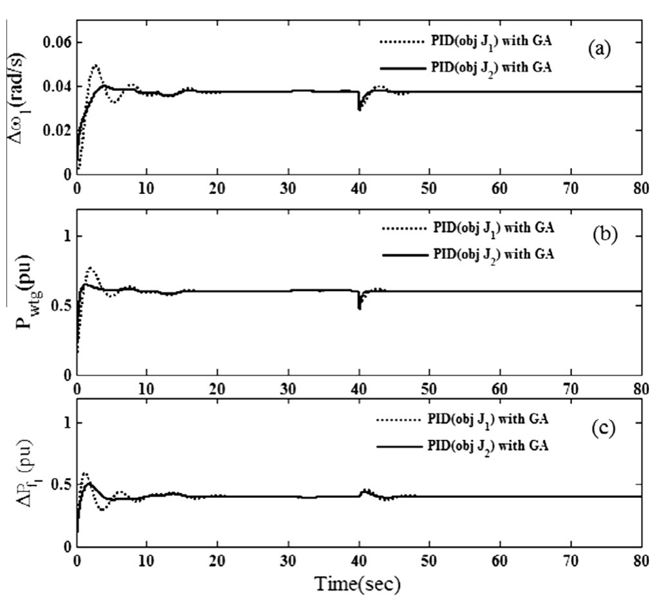

Fig. 7. Dynamic responses for (a) WTG frequency deviation, (b) WTG power output and (c) diesel generator power output considering optimum value of P–I–D gain parameters optimized by GA using fitness functions given by Eqs. (28) and (30).

Table 5
Optimized P–I and P–I–D gain parameters considering fitness function given by Eq. (28) using PSO.

Control schemes	Optimum gains	Objective function (J_1)
P–I	K_1 = 50.93 K_2 = 74.23	0.4960
P–I–D	K_1 = 96.67 K_2 = 116.39 K_3 = 66.82	0.5381

using PSO and the optimum values of gain parameters are more or less same for $0 \leqslant P_{max} \leqslant 0.6$. From Table 6, it is observed that the value of J_2 with optimum P–I–D controller is much lower than that obtained with optimum P–I controller. Tables 7 and 8 gives the eigenvalues of the system without any controller, with optimum P–I and P–I–D controllers considering the gain values obtained using PSO given in Tables 5 and 6 respectively.

Fig. 8(a)–(c) show the dynamic responses for WTG frequency deviation, WTG power output and diesel generator power output considering the optimum P–I and P–I–D gain parameters given in Table 5. These responses are obtained for the same base, gust ramp and noise wind conditions and for the same loading conditions as discussed in Section 'Performance of GA based P–I and P–I–D controllers'. It is seen from Fig. 8(a) and (c) that the peak value of WTG frequency deviation and peak value of diesel power deviation with P–I–D controller is more than that obtained with

Table 6
Optimized P–I and P–I–D gain parameters considering fitness function given by Eq. (30) using PSO.

Control schemes	Optimum gains	Objective function (J_2)
P–I	K_1 = 139.74 K_2 = 11.21	20.14
P–I–D	K_1 = 198.14 K_2 = 147.39 K_3 = 29.68	11.28

Table 7
Eigenvalues of the wind–diesel system using PSO with J_1.

Eigenvalues without controller	Eigenvalues with P–I controller	Eigenvalues with P–I–D controller
	$F_1 = J_1$ (Eq. (28))	$F_1 = J_1$ (Eq. (28))
−39.0283	−39.0281	−39.0377
−24.3995	−24.8195	−13.4040 ± 13.8191i
−3.4191	−0.6182 ± 2.6498i	−1.6241
−1.0408 ± 0.2401i	−2.1953	−0.5381 ± 1.0172i
−0.3467 ± 0.7300i	−1.3512	−0.5382 ± 0.9084i
–	−0.4960 ± 0.8911i	–

Table 8
Eigenvalues of the wind–diesel system using PSO with J_2.

Eigenvalues without controller	Eigenvalues with P–I controller	Eigenvalues with P–I–D controller
	$F_2 = J_2$ (Eq. (30))	$F_2 = J_2$ (Eq. (30))
−39.0283	−39.0275	−39.0330
−24.3995	−25.5606	−18.1849
−3.4191	−1.1654 ± 4.9765i	−4.4315 ± 4.7222i
−1.0408 ± 0.2401i	−1.6989	−1.7433
−0.3467 ± 0.7300i	−0.4639 ± 0.8758i	−0.4736 ± 0.8777i
–	−0.0768	−0.8511

P–I controller. For wind power deviation (Fig. 8(b)) peak value is slightly less with P–I–D controller than that obtained with P–I controller. But in the case of ramp wind disturbance the dynamic responses (Fig. 8(a)–(c)) with P–I–D controller is much superior than that obtained with P–I controller in terms of peak deviation.

Fig. 9(a)–(c) show the dynamic responses for WTG frequency deviation, WTG power output and diesel generator power output considering the optimum P–I and P–I–D gain parameters given in Table 6 under similar conditions as mentioned above. From Fig. 9(a)–(c), it is seen that the P–I–D controller gives much better dynamic responses. Fig. 10 shows the dynamic performances considering optimum P–I–D gain parameters (Table 5) obtained by maximizing the degree of stability and optimum P–I–D gain Parameters (Table 6) obtained by minimizing quadratic objective function. From Fig. 10, it is seen that the dynamic responses are better in terms of peak deviation considering optimum gain settings of P–I–D controller (see Table 6) obtained by minimizing the quadratic objective function.

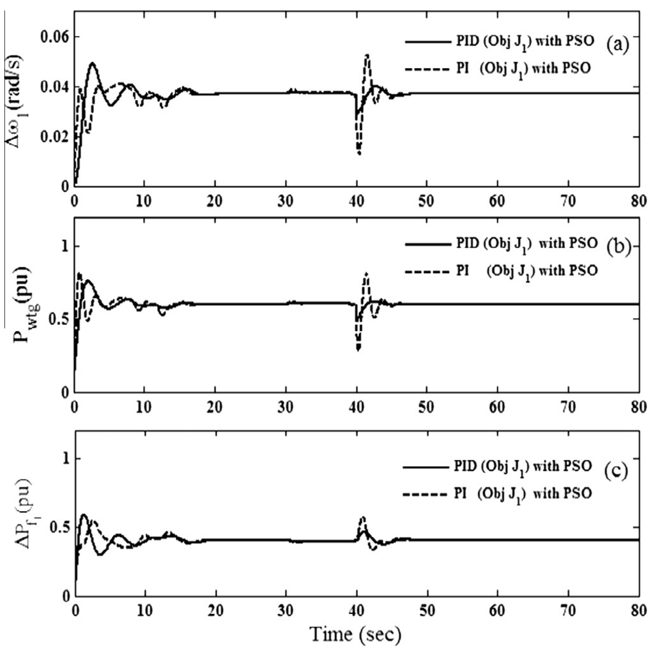

Fig. 8. Dynamic responses for (a) WTG frequency deviation, (b) WTG power output and (c) diesel generator power output considering optimum value of P–I and P–I–D gain parameters using PSO (Table 5).

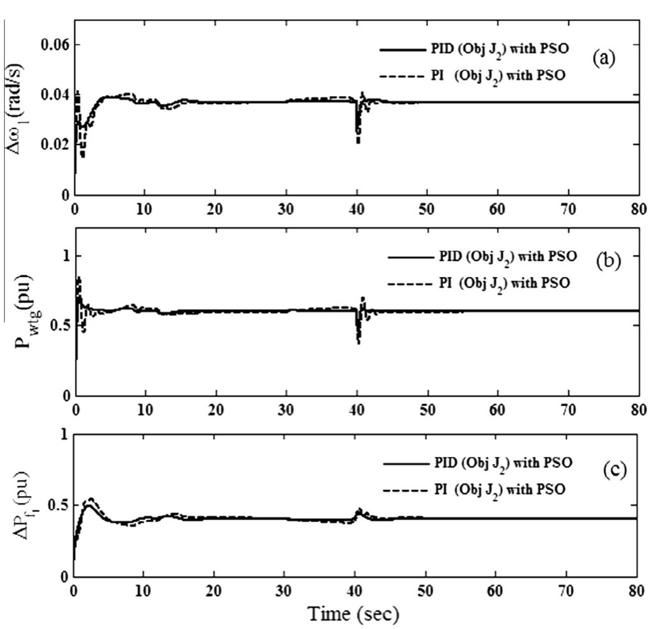

Fig. 9. Dynamic responses for (a) WTG frequency deviation, (b) WTG power output and (c) diesel generator power output considering optimum value of P–I and P–I–D gain parameters using PSO (Table 6).

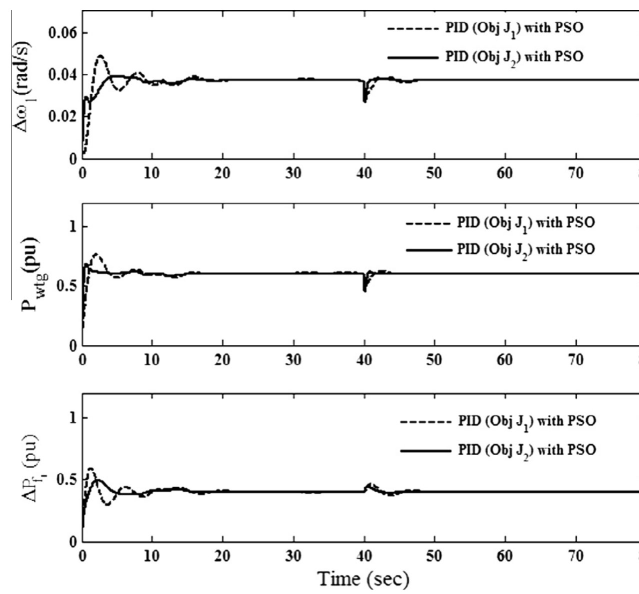

Fig. 10. Dynamic responses for (a) WTG frequency deviation, (b) WTG power output and (c) diesel generator power output considering optimum value of P–I–D gain parameters optimized by PSO using fitness functions given by Eqs. (28) and (30).

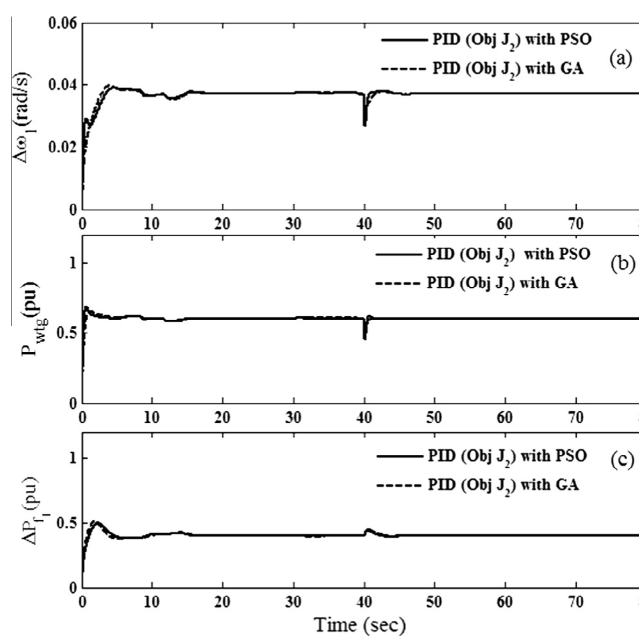

Fig. 11. Comparison of dynamic responses for (a) WTG frequency deviation, (b) WTG power output and (c) diesel generator power output considering optimum value of P–I–D gain parameters optimized by PSO and GA using fitness function given by Eq. (30).

Comparison of performance of GA and PSO based P–I and P–I–D controllers

The GA and PSO algorithms are executed using MATLAB 2007a software on a Pentium dual core CPU with 3.2 GHz speed and 2 GB RAM computer. From Figs. 5–11, it can be observed that the dynamic responses obtained by P–I controller gains optimized by GA and PSO techniques and the dynamic responses obtained by GA and PSO based P–I–D controllers have similar characteristics. However, computationally PSO is more efficient than GA.

Table 9 shows the parameters for comparing the performance of GA and PSO techniques. From Table 9 it can be observed that for finding optimum gains of P–I controller and P–I–D controller using objective function J_1, the time of execution for implementing PSO algorithm is taking less time of execution compared to that of GA algorithm for the same number of population and generations. In the case of optimization of gains for the P–I and P–I–D controllers using objective function J_2 the PSO technique is giving better results compared to GA with less number of population size and computation time. Hence it can be said that PSO technique is efficient compared to GA technique for obtaining optimum P–I and P–I–D controllers gains for wind diesel system.

Table 10 depicts the dynamic response specifications, overshoot, settling time and damping ratio for WTG frequency deviation, WTG power output and diesel generator power output for PSO based P–I and P–I–D controllers. From Table 10 it can be said that the P–I–D controller optimized using PSO with objective function J_2 has better dynamic responses in terms of minimum overshoot and optimum settling time compared to all other cases with reasonably good damping ratio. From the above analysis it can be concluded that the P–I–D controller optimized using PSO technique with quadratic objective function J_2 is superior to all other cases.

Sensitivity analysis of wind diesel system

Sensitivity analysis is performed to study the effect of variations in the system parameters on the dynamic responses of wind diesel system [17–20]. Since the performance of the PSO based P–I–D controller optimized by objective function J_2 is superior to all other cases, it used to carry sensitivity analysis of the system. The system

Table 9
Comparison of performance of GA and PSO techniques for P–I and P–I–D controller.

Performance index	P–I controller				P–I–D controller			
	(Obj. J_1)		(Obj. J_2)		(Obj. J_1)		(Obj. J_2)	
	GA	PSO	GA	PSO	GA	PSO	GA	PSO
No of generations	20	20	20	20	20	20	20	20
Population size	500	500	100	50	500	500	100	50
Magnitude	0.4959	0.4960	20.52	20.14	0.5322	0.5381	12.85	11.28
Time of execution	0.60 s	0.37 s	76.47 s	38.10 s	0.60 s	0.37 s	76.82 s	38.26 s

Table 10
Dynamic response specifications for PSO based P–I and P–I–D controllers.

Type of controller	Overshoot (Mp) (pu)			Settling time (Ts) (s)			Damping ratio
	$\Delta\omega_1$	P_{wtg}	ΔP_{f_1}	$\Delta\omega_1$	P_{wtg}	ΔP_{f_1}	
P–I (Obj. J_1)	0.017	0.224	0.175	16.92	15.00	17.66	0.4864
P–I–D (Obj. J_1)	0.012	0.164	0.192	17.47	15.00	18.39	0.5097
P–I (Obj. J_2)	0.005	0.249	0.143	17.76	15.00	17.06	0.4681
P–I–D (Obj. J_2)	0.002	0.088	0.096	16.75	15.00	15.30	0.4749

Table 11
Sensitivity analysis of wind diesel hybrid system.

Parameter variation	% Change	Overshoot (Mp) (pu)			Settling time (Ts) (s)			Damping ratio	Obj. J_1	Obj. J_2
		$\Delta\omega_1$	P_{wtg}	ΔP_{f_1}	$\Delta\omega_1$	P_{wtg}	ΔP_{f_1}			
Nominal	0	0.002	0.088	0.096	16.75	15.00	15.30	0.4749	0.4736	11.28
H_w	+25	0.002	0.107	0.095	16.74	15.00	15.30	0.4735	0.4737	12.10
	−25	0.002	0.065	0.097	16.74	15.00	15.30	0.4762	0.4735	10.42
H_d	+25	0.003	0.097	0.112	15.00	15.00	15.41	0.4239	0.3755	11.75
	−25	0.001	0.073	0.078	16.48	15.00	15.11	0.5516	0.6452	10.62
K_d	+25	0.001	0.087	0.081	16.32	15.00	15.15	0.5343	0.5999	11.34
	−25	0.004	0.089	0.117	17.31	15.00	15.42	0.4087	0.3508	11.23
K_{pc}	+25	0.002	0.080	0.096	15.00	15.00	15.21	0.4761	0.4736	10.30
	−25	0.002	0.094	0.096	17.03	15.00	15.39	0.4723	0.4734	12.85
K_{hp_2}	+25	0.002	0.080	0.096	15.00	15.00	15.21	0.4760	0.4736	10.30
	−25	0.002	0.093	0.096	17.03	15.00	15.39	0.4726	0.4734	12.85
K_{hp_3}	+25	0.002	0.080	0.096	15.00	15.00	15.21	0.4760	0.4736	10.30
	−25	0.002	0.094	0.096	17.05	15.00	15.39	0.4726	0.4734	12.85
T_{hp_1}	+25	0.002	0.073	0.097	15.00	15.00	15.41	0.4735	0.4714	10.38
	−25	0.002	0.109	0.095	16.65	15.00	15.17	0.4768	0.4760	12.70
T_{hp_2}	+25	0.002	0.094	0.096	16.74	15.00	15.29	0.4750	0.4737	11.56
	−25	0.002	0.083	0.096	16.79	15.00	15.31	0.4747	0.4734	11.02
T_1	+25	0.002	0.088	0.097	16.78	15.00	15.30	0.4729	0.4731	11.27
	−25	0.002	0.088	0.095	16.77	15.00	15.29	0.4767	0.4739	11.29

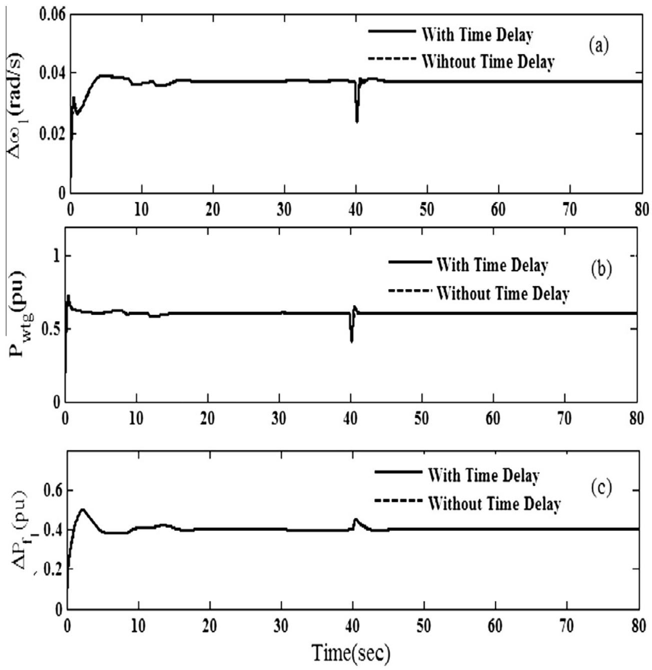

Fig. 12. Comparison of dynamic responses for (a) WTG frequency deviation, (b) WTG power output and (c) diesel generator power output, with and without time delay incorporation considering optimum value of P–I–D gain parameters optimized by PSO using fitness function given by Eq. (30).

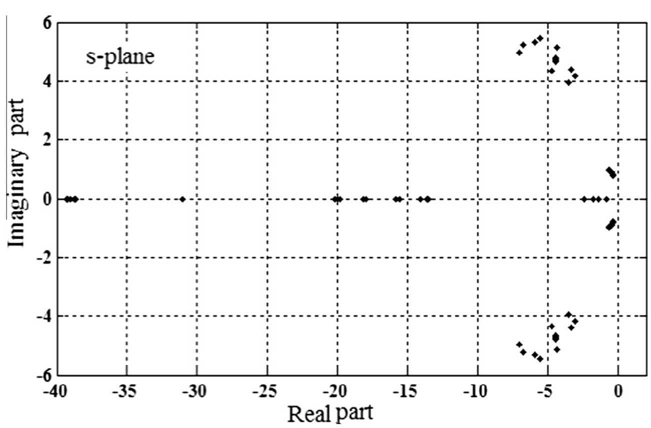

Fig. 13. Eigenvalues of wind diesel system with parameter variations.

parameters are changed by ±25% from their nominal values taking one at a time and the overshoot, settling time (2%), minimum damping ratio and objective functions J_1 and J_2 are calculated and the results are given in Table 11. From Table 11 it is clear that the effect of variations on system parameters is negligible on the performance of the wind diesel system. The variations in fluid coupling coefficient (K_{fc}) directly effect the wind turbine generator power out put and hence it must be maintained constant for efficient operation of wind diesel hybrid system. A time delay (T_d) of 50 ms is incorporated into the wind diesel system MATLAB simulink model to find the effect of time delay on the dynamic responses of the system.

Fig. 12 gives the comparison of dynamic responses of the system with and without time delay considering PSO based PID controller obtained using objective function J_2. From Fig. 12, it is seen that the effect of time delay on the dynamic responses of the wind diesel system is negligible.

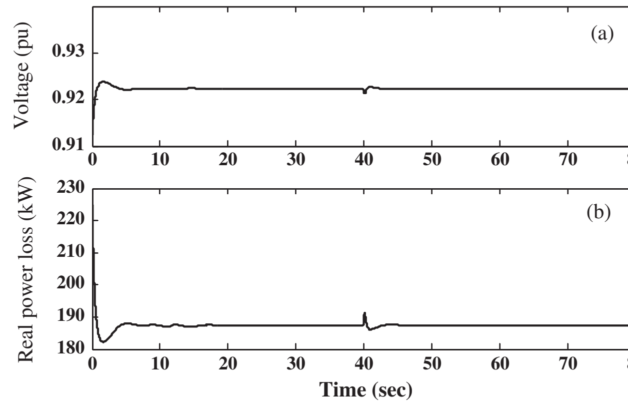

Fig. 14. Variations of voltage magnitude of node 61 and real power loss during power injection by wind–diesel hybrid system into the 69 node distribution work.

Stability analysis of wind diesel system

In the literature various robust control design techniques have been proposed to deal the load frequency control problem for stable operation of distribution power generation systems under disturbance conditions [21]. The closed loop system stability is guaranteed if all the eigenvalues are located to the left half of the s-plane [22]. The system is said to be D-stable if all the eigenvalues of the system matrix have negative real parts. The closed loop system is said be robustly D-stable if all the eigenvalues of the closed loop system matrix corresponding to the parameter variations strictly lies on the left half of the s-plane [23,24]. The wind diesel system is a closed loop system with the P–I–D controller.

Fig. 13 gives the plot of eigenvalues corresponding to all the parameter variations mentioned in Table 11. From Fig. 13 it can be observed that all the eigenvalues corresponding to parameter variations are located on the left half of the s-plane and hence it is clear that the closed loop system with the proposed PSO based P–I–D controller optimized using objective function J_2 is robustly stable according to D-stability criterion.

Effect of power injection by wind–diesel hybrid system on distribution network

In this case, power injection of wind diesel system on a sixty-nine node distribution network is examined. Data for the sixty-nine node distribution network is available in [25]. Wind–diesel system is connected at node 61. Total power injection by wind–diesel system was set to 250 kW. Out of which WTG system is set to generate 150 kW (i.e., P_{max} = 150 kW) and surplus is generated by diesel generator. Other conditions are same as mentioned in Section 'Gain parameters optimization of P–I and P–I–D controllers using PSO'. In this case, in every iteration of solving state space equation (Eq. (13)), total wind and diesel power is injected at node 61 and load flow run was carried out to get the voltage and power loss variation with time.

Fig. 14(a) shows the transient behavior of voltage magnitude of node 61. Before power injection $|V_{61}|$ = 0.9123 pu and after power injection steady state value of $|V_{61}|$ = 0.9223 pu. Similarly, Fig. 14(b) shows the transient behavior of real power loss. Before power injection, it was 224.94 kW and after power injection, steady state value of real power loss is 187.35 kW.

Conclusions

In this paper dynamic performances of an isolated wind–diesel hybrid power system has been studied considering P–I and P–I–D controllers. Complete wind model has also been incorporated in this study. Gain parameters of P–I and P–I–D controllers have been optimized by using genetic algorithm and particle swarm optimization considering eigenvalue based objective function and quadratic objective function. Analysis reveals that the gain parameters optimized using particle swarm optimization and genetic algorithm give more or less similar dynamic responses. However, it was found that particle swarm optimization is computationally more efficient than genetic algorithm. It was also observed that the effect of wind noise on dynamic performances is negligible and may be neglected from the mathematical model. The sensitivity analysis has also been carried out to demonstrate the robustness of the closed loop system to parameter variations. The closed loop system is shown robustly stable according to D-stability criterion. Finally the effect of power injection by wind–diesel hybrid system on a distribution network was examined and its performance was found to be satisfactory.

Appendix A

System Data [1,3,6]

Base value = 250 kVA
Wind system Inertia constant (H_w) = 3.52 s
Diesel system Inertia constant (H_d) = 8.7 s
$MGWS$ = 12 m/s
$MRWS$ = 10 m/s
V_{WB} = 7 m/s
K_{fc} = 16:2 pu kW/Hz
$K_{hp_2} = 1.25$
K_d = 16.5 pu kW/Hz
$K_{hp_3} = 1.40$
$T_{hp_1} = 0.60$ s
$T_{hp_2} = 0.041$ s
$P_{\max}$ = 0.6
P_{load} = 1.0 pu
K_{pc} = 0.080
T_1 = 0.025 s
$\Delta\omega_{ref}$ = 0.0
Surface drag coefficient (K_N) = 0.004
Turbulence scale (F) = 2000 m
Mean speed of wind (μ) = 7.5 m/s
$\Delta\Omega$ = 0.5–2.0 rad/s.

References

[1] Scott GW, Wilreker VF, Shaltens RK. Wind turbine generator interaction with diesel generators on an isolated power system. IEEE Trans Power Appar Syst 1984;103(5):933–7.
[2] Kamwa I. Dynamic modeling and robust regulation of a no-storage wind–diesel hybrid power system. Electr Power Syst Res 1990;18(3):219–33.
[3] Tripathy SC, Kalantar M, Balasubramanian R. Dynamics and stability of wind and diesel turbine generators with superconducting magnetic energy storage unit on an isolated power system. IEEE Trans Energy Convers 1991;l6(4):579–85.
[4] Stavrakakis GS, Kariniotakis GN. A general simulation algorithm for the accurate assessment of isolated diesel wind turbines system interaction: Part I: general multi machine power system model. IEEE Trans Energy Convers 1995;10(3):577–83.
[5] Kariniotakis GN, Stavrakakis GS. A general simulation algorithm for the accurate assessment of isolated diesel–wind turbines systems interaction. Part II: implementation of the algorithm and case-studies with induction generators. IEEE Trans Energy Convers 1995;10(3):584–90.
[6] Das D, Aditya SK, Kothari DP. Dynamics of diesel and wind turbine generators on an isolated power system. Int J Electr Power Energy Syst 1999;21(3):183–9.
[7] Chedid RB, Karaki SH, El-Chamali C. Adaptive fuzzy control for wind diesel weak power systems. IEEE Trans Energy Convers 2000;15(1):71–8.
[8] Papathanassiou SA, Papadopoulos MP. Dynamic characteristics of autonomous wind–diesel systems. Renew Energy 2001;23(2):293–311.
[9] Gaing Z. A particle swarm optimization approach for optimum design of PID controller in AVR system. IEEE Trans Energy Convers 2004;19(2):384–91.
[10] Tan W. Tuning of PID load frequency controller for power systems. Energy Convers Manage 2009;50(6):1465–72.
[11] Khodabakhshian A, Hooshmand R. A new PID controller design for automatic generation control of hydro power systems. Int J Electr Power Energy Syst 2010;32(5):375–82.
[12] Mostafa H, El-Sharkawy M, Emary A, Yassin K. Design and allocation of power system stabilizers using the particle swarm optimization technique for an interconnected power system. Int J Electr Power Energy Syst 2012;34(1):57–65.
[13] Anderson PM, Bose A. Stability and simulation of wind turbine system. IEEE Trans Power Appar Syst 1983;102(12):3791–5.
[14] Grefenst JJ. Optimization of control parameters for genetic algorithms. IEEE Trans Syst Man Cybern 1986;16(1):122–8.
[15] Goldberg DE. Genetic algorithms in search, optimization and learning. A book. Reading, MA: Addision-Wesley; 1989.
[16] Kennedy J, Eberhart R. Particle swarm optimization. In: Proceedings of IEEE international conference on neural networks (ICNN), vol. 4; 1995. p. 1942–8.
[17] Rout UK, Sahu RK, Panda S. Design and analysis of differential evolution algorithm based automatic generation control for interconnected power system. Ain Shams Eng J 2013;4(3):409–21.
[18] Gozde HM, Cengiz TM, Kocaarslan I. Comparative performance analysis of artificial bee colony algorithm in automatic generation control for interconnected reheat thermal power system. Int J Electr Power Energy Syst 2012;42(1):167–78.
[19] Singh Parmar KP, Majhi S, Kothari DP. Load frequency control of a realistic power system with multi source power generation. Int J Electr Power Energy Syst 2012;42(1):426–33.
[20] Singh VP, Mohanty SR, Kishor N, Ray PK. Robust H-infinity load frequency control in hybrid distributed generation system. Int J Electr Power Energy Syst 2013;46:294–305.
[21] Pandey SK, Mohanty SR, Kishor N. A literature survey on load-frequency control for conventional and distribution generation power systems. Renew Sust Energy Rev 2013;25:318–34.
[22] Tripathy SC. Dynamic simulation of hybrid wind–diesel power generation system with superconducting magnetic energy storage. Energy Convers Manage 1997;38(9):919–30.
[23] Abed EH. Strong D-stability. Syst Control Lett 1986;7(3):207–12.
[24] Singh Ravindra. A novel approach for tuning of power system stabilizer using genetic algorithm. M.E. thesis submitted to Department of Electrical Engineering, Indian Institute of Science, Bangalore, India; 2004.
[25] Chakravorty M, Das D. Voltage stability analysis of radial distribution networks. Int J Electr Power Energy Syst 2001;23(2):129–35.